The 11th Canadian Conference on Earthquake Engineering
Canadian Association for Earthquake Engineering

SEISMIC PERFORMANCE OF CONCRETE COLUMNS REINFORCED WITH HIGH-STRENGTH STEEL

Drit Sokoli
PhD Student, The University of Texas at Austin, USA
drit@utexas.edu

Wassim M. Ghannoum
Assistant Professor, The University of Texas at Austin, USA
ghannoum@mail.utexas.edu

ABSTRACT: Test results are presented from an experimental program conducted to evaluate the seismic performance of concrete columns reinforced with high-strength steel. Comparisons are made between the performance of columns reinforced with conventional 420 MPa steel (Grade 60), and the higher 550 MPa (Grades 80) and 690 MPa (Grade 100). The high-strength steel used in this study is the result of a recent push by U.S. manufacturers to produce higher grade reinforcing bars with relatively high ductility. The 690 MPa (Grade 100) bars used in this study have only become possible in the last year and boast a well-defined yield point and fracture elongation strains of 10 to 14%. Column specimens were tested under constant axial load and reverse cyclic lateral loading until severe degradation. A high-resolution digital image correlation system developed by the authors was used to measure surface deformations. The system allowed detailed comparisons of deformations, strains, cracks, and damage between test specimens. Conclusions are drawn with respect to the effects of higher strength reinforcement on the seismic performance of concrete columns and strain demands on reinforcing bars.

1. Introduction

In this study, high-strength steel refers to reinforcing steel having a yield strength of 550 MPa (80 ksi) or more. The production of high strength steel in the United States has seen major developments in the last three years, with manufacturers now producing reinforcing bars with strength as high as 830 MPa (120 ksi), a well-defined yield plateau, and fracture elongation strains above 10%. The newly developed reinforcing steel grades have prompted a large national effort to explore the potential introduction of such steel grades into design codes. High strength steel has the potential to reduce substantially the overall volumes of steel installed by the construction industry, with associated cost savings and reductions in energy and raw material consumption.

In many cases, current U.S. codes limit the strength of reinforcing steel used in concrete members to 420 MPa (60 ksi). These limits on strength of concrete reinforcing steel have been enforced since the 1950s when the limit was increased from 275 MPa to 420 MPa (40 ksi to 60 ksi). To this date, the limit of 550 MPa (80 ksi) is applied to all non-seismic systems except for shear, which has to be designed using maximum yield strength of transverse reinforcement of 420 MPa (60 ksi) (ACI 318-14, 2014). The limit of 420 MPa (60 ksi) remains for all bars in seismic design (ACI 318-14) except confining bars, for which a yield strength of 690 MPa (100 ksi) is permitted.

Various concerns related to the performance of concrete members reinforced with high strength steel have hindered its incorporation into building codes. The increase in steel strength in reinforcing bars is associated with an increase in the strain at yield, and often with a reduction in the fracture elongation, the tensile-to-yield strength ratio, and the length of the yield plateau. For a given bar size, higher forces are required in the high-strength bar in order to utilize its strength, thus leading to larger tensile and compressive forces. Larger tensile forces result in an increase in bond demands and the forces at bar hooks. Larger compressive forces can make the same bar size more prone to buckling given the same

lateral bracing. These can result in the member having a lower deformation capacity. In the serviceability range, larger strains at service loads can lead to increase crack widths and deflections. Larger crack widths in turn can lead to the weakening of the concrete shear-transfer mechanisms and lower shear strengths.

An experimental program was carried out to investigate the ability of high-strength reinforcing bars (HSRB) to maintain the integrity of shear transfer mechanisms at large deformation demands during seismic events. Three full-scale concrete columns, each reinforced with a different grade of steel and satisfying most of the provisions of ACI 318-14 for Special Moment Resisting Frames were tested under constant axial load and cyclic lateral loading until loss of axial strength or residual lateral strength. Column CS60 and CS80 were respectively reinforced with bars having a yield strength of 420 MPa (Grade 60) and 550 MPa (Grade 80) longitudinal and transverse reinforcement satisfying ASTM A706 specifications. The third column was reinforced with newly developed high-strength reinforcing bars with relatively high fracture elongations. Longitudinal bars in the third column had a yield strength exceeding 690 MPa (100 ksi), which were dubbed Grade 100 bars, while transverse bars had a yield strength slightly below 830 MPa (120 ksi) and were dubbed as Grade 120 bars. The columns were designed to impart large demands on the transverse reinforcement. Columns were subjected to large shear stresses generated by a high longitudinal reinforcement ratio, and large confinement demands generated by a relatively large compressive axial load.

2. Experimental Program

The experimental program consisted of three geometrically identical columns. They were tested under constant compressive axial load and quasi-static reversed cyclic lateral loading until loss of axial strength or residual lateral strength. Column CS60 was reinforced exclusively with Grade 60 (420 MPa) ASTM A706 (2014) bars. Column CS80 was reinforced exclusively with Grade 80 (550 MPa) A706 (2014) bars, while column CS100 was reinforced with newly developed Grade 100 (690 MPa) longitudinal bars and Grade 120 (830 MPa) transverse hoops. Columns were identical with the only variable being the grade of steel used. As the reinforcement was pushed to higher grades, the bar size was reduced leading to an almost constant $A_s f_y$ (where A_s is the total cross-sectional area of longitudinal reinforcement and f_y is the yield strength) in all cases. All columns were designed to have almost identical flexural capacity and associated shear demands. All columns had the same layout of longitudinal and transverse reinforcement (except that hoops were spaced one inch tighter in CS100). All columns had the same concrete mix design and were tested under the same loading protocol. Columns were designed and detailed to satisfy most of the seismic provisions for Special Moment Resisting Frames of ACI 318-14 (2014). The hoop spacing in CS60 and CS80 exceeded by one inch the maximum allowed spacing in ACI 318-14 for confinement of plastic hinge regions. CS100 met the hoop spacing limit. The shear contribution of transverse reinforcement exceeded the $0.67\sqrt{f_c'}$ in MPa units ($8\sqrt{f_c'}$ in psi units; where f'_c is concrete compressive strength) limit imposed in ACI 318-14. The hoop design was governed by shear and not confinement requirements.

2.1. Specimen Design

Concrete compressive strength of 31 MPa (4500 psi) was specified for all three specimens. Figure 1 shows a typical cross sectional view of the specimens. All specimens had the same cross-sectional layout and only the bar size was reduced as higher strength reinforcement was used. All columns had 12 longitudinal bars distributed evenly along all four faces (Figure 1). Column CS60 had 12 #10 (32 mm) longitudinal bars, column CS80 had 12 #9 (29 mm) longitudinal bars, and column CS100 had 12 #8 (25 mm) bars. The full-scale column specimens had a clear height of 2134 mm (84 in.) and cross-sectional dimensions of 457x457 mm (18x18 in.), with a clear cover of 38 mm (1.5 in.) (Figure 1). Splices were not part of this investigation, thus none of the specimens contained splices. Ample embedment depth was provided for all bars in the footing. The shear span-to-depth ratio was about 2.7 for all columns. Columns framed into two footings, which were much stronger and stiffer than the columns.

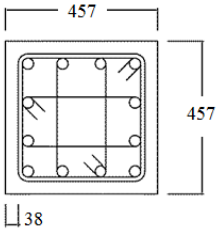

Figure 1 – Cross sectional view of the specimens (Units: mm)

The transverse reinforcement consisted of three closed hoops spaced on center at 140 mm (5.5 in) for CS60 and CS80, and 114 mm (4.5 in.) for CS100. Hoop details met the extension and bar bend requirements of hoops defined in ACI 318-14. Since hoop design was governed by shear, which was constant over column height, hoops spacing was maintained over column height. Reinforcement details as well as the longitudinal and transverse steel ratios (ρ_l and ρ_r respectively) are presented for all columns in Table 1. The spacing to bar-diameter (d_b) ratio was similar for all three specimens.

Table 1 – Design quantities

	CS60	CS80	CS100
Longitudinal reinforcement	12 #10 (32mm) ρ_l = 4.7%	12 #9 (29mm) ρ_l = 3.7%	12 #8 (25mm) ρ_l = 2.9%
Transverse reinforcement	4 #5 legs (16 mm) @5.5in. (140mm) ρ_r = 1.50% 4.4 d_b	4 #4 legs (13 mm) @5.5in. (140mm) ρ_r = 0.94% 4.9 d_b	4 #3 legs (10 mm) @4.5in. (114mm) ρ_r = 0.65% 4.5 d_b

The sectional analyses performed at the design stage accounted for a compressive axial load of 1646 kN (370 kips). Based on the design compressive strength of 31 MPa (4500 psi) the resulting design axial load ratio was $0.27 A_g f_c'$ (with A_g = gross sectional area). The sectional analysis gave a plastic moment strength (M_{pr}) for all three columns of about 850 kN-m (7,500 kip-in.), which resulted in a corresponding peak shear demand (V_e) of 792 kN (178 kips). The expected peak shear stress (V_e/bd where b = width of the section and d = the depth of the section) was therefore $0.8\sqrt{f_c'}$ in MPa units ($9.6\sqrt{f_c'}$ in psi units) for all columns. As flexural yielding was intended in the tests, the shear strength of the column was designed to be larger than V_e/φ (with φ = 0.75 as per ACI 318-14). The steel contribution to shear strength (V_s) exceeded the ACI 318-14 limit of $0.67\sqrt{f_c'}$ in MPa units ($8\sqrt{f_c'}$ in psi units).

2.2. Test Setup

Specimens were tested under symmetric double curvature with fixed rotation boundary conditions at both ends. Quasi-static cyclic loading in a single direction as well as a constant axial load of 1646 kN (370 kips) were applied using three hydraulic actuators (Figure 2). The lateral loading protocol consisted of two lateral displacement cycles at increasing target drifts as suggested by FEMA 461 (2007). The targeted lateral drift ratios (the ratio of lateral drift to column clear height) were: 0.2%, 0.3%, 0.4%, 0.6%, 0.8%, 1.0%, 1.5%, 2.0%, 3.0%, 4.0%, 5.5%, and 7.0%. Tests were carried out in displacement control under small loading rates.

2.3. Instrumentation and Data Processing

Columns were instrumented to measure the applied loads, deformations throughout the height of the members, and strains in the reinforcing bars. Two linear potentiometers were used to measure column lateral drifts during testing. The vertical movement of the steel frame at the point of connection with the horizontal actuator was measured in order to estimate the applied forces on the column. Large-deformation equilibrium accounting for the location and inclination of all three actuators was used to calculate the forces acting on the column.

Strain in reinforcing bars was measured with strain gauges, which were installed on transverse hoops within the top and bottom plastic hinge regions. Strain gauges were also installed on the corner longitudinal bars at both ends of the columns, where strain demands were expected to be the highest.
A Digital Image Correlation (DIC) system developed by the authors was used to measure column surface deformations, from which surface strains and crack widths were obtained (Sokoli et. al., 2014). The DIC system was able to resolve footing deformations on the order of a 1/100th of a pixel, which is equivalent to 1/10,000th of an inch over the field of view.

Figure 2 – Column CS100 during testing

For 3D measurements, the DIC system uses two cameras that record images of the surface of interest from different angles (Figure 2). A rectangular grid of targets was placed on the surface of the column. Through the process of digital image correlation the coordinates of each target were obtained throughout the tests. By triangulation using data from the two cameras, the three-dimensional coordinates of all targets were obtained for each pair of captured image frames. Lens distortion was accounted for through a calibration process.
Column deformations presented in this paper were all extracted from DIC data. The lateral drift of the columns was obtained by averaging the horizontal displacements of all available targets on the top footing and subtracting from them the average horizontal displacement of all available targets on the bottom footing. While the bottom footings did not slide during the test, this procedure removed any footing deformations from the column deformation data.
Target displacement data from the DIC system were used to get rotations, curvatures, and deformation components at each row of targets over the height of the specimens, as described in Sokoli et. al. (2014). The surface targets arranged in a rectangular mesh were used as nodal points for bilinear quadrilateral elements. Contour plots showing the x-directional or horizontal strains (ε_x), the y-directional or vertical strains (ε_y), and the principal strains (ε_1 = largest principal strain and ε_2 = smallest principal strain) element strains were produced assuming that strains vary linearly between two nodal points (Sokoli et. al., 2014).

2.4. Material Properties

Concrete strength was measured using three cylinder tests per cast as per ASTM C39 (2014). The three-cylinder average concrete compressive strengths at column testing were 26.4 MPa (3.83 ksi) for column CS60, 28.8 MPa (4.18 ksi) for column CS80, and 32 MPa (4.65 ksi) for column CS100.
Three bar coupons per bar size and grade were tested monotonically in tension to fracture as per ASTM A370 (2014). The same DIC system used for monitoring column deformations and strains was used to measure strains at an eight-inch gauge length along the length of the steel coupons. Table 2 summarizes the average results from the measured quantities for three coupons for each steel grade and bar size. The fracture and uniform elongations decreased as the yield strength increases. Uniform elongation is the bar elongation at peak stress. The higher grade bars did however achieve relatively high uniform elongations and were at most 20% lower than Grade 60 (420 MPa) values (Table 2). The tensile-to-yield strength ratio also (T/Y ratio) gradually decreased as the yield strength increased and ranged from 1.41 for #10 (32 mm) Grade 60 (420 MPa) bars to 1.18 for #3 (10 mm) Grade 120 (830 MPa) bars (Table 2). Typical stress-strain relations for the bars used in columns are presented in Figure 3 . All steel stress-strain curves had a similar shape, with nearly linear behavior up to yielding and a well-defined yield plateau. A decrease in the yield plateau length was observed for the higher steel grades.

Table 2 – Average bar mechanical properties

Bar Size	Grade in ksi (MPa)	Yield Strength, ksi (MPa)	Tensile Strength, ksi (MPa)	Fracture to Yield Ratio	Fracture Elongation (%)	Uniform Elongation (%)
#10	60 (420)	67.3 (464)	94.9 (654)	1.41	18.3	10.1
#9	80 (550)	79.1 (545)	106.5 (734)	1.34	15.5	8.8
#8	100 (690)	101.5 (700)	128.5 (886)	1.26	11.6	8.3
#5	60 (420)	68.5 (472)	95.8 (660)	1.40	14.4	9.9
#4	80 (550)	83.7 (577)	111.4 (768)	1.33	12.1	8.9
#3	100 (830)	118.9 (820)	141.0 (972)	1.18	10.1	8.4

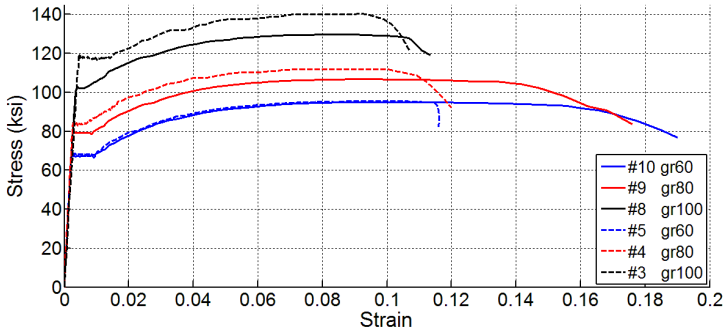

Figure 3 – Stress-strain curves from bar coupons

3. Column Behavior

The damage progression in the column specimens is presented through the following major behavioral milestones: the first longitudinal reinforcement yield, the first transverse reinforcement yield, the first inclined crack, the first flexural crack, the peak lateral load, the initiation of lateral-strength loss, and the initiation of axial failure. A legend of the behavioral milestones is given in Figure 4. These milestones are identified on the column lateral load (V) versus lateral drift relations in Figures 5 and 7. The first longitudinal reinforcement yield was determined from strain gauges at the column/footing interfaces where the strain demands were expected to be the highest. The first transverse reinforcement yield was obtained from DIC strain data (x-direction strains). First cracking was obtained from DIC data by identifying the first elements whose principal tensile strains had a sudden jump past the cracking strain. Differentiation between flexural and inclined cracks was made through the angle of the principal strains. The peak lateral load, the initiation of lateral-strength loss, and the initiation of axial failure were identified using actuator load cell data.

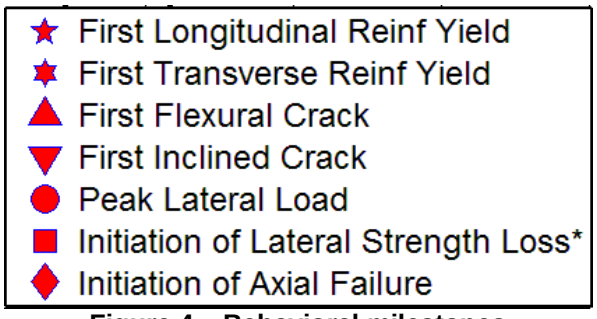

Figure 4 – Behavioral milestones

**Initiation of lateral strength loss was due shear failure in CS60 and CS80 or bond failure in CS100.*

3.1. Overall Behavior

Columns CS60 and CS80 showed comparable responses up to initiation of lateral-strength loss, which occurred beyond the second excursion to a lateral drift ratio of +5.5% (Figure 5).

Column CS60 initiated loss of lateral strength at a drift ratio of +5.2% as the column was being pushed to the first excursion to a drift ratio of +7.0%. The initiation of lateral-strength loss was associated with opening of large shear cracks, which lead to the reduction in lateral load resistance. Column CS60 started losing axial capacity shortly after, at a drift ratio of +5.8%. Beyond initiation of axial failure, the column was no longer able to resist the target axial load of 1646 kN (370 kips) and that load was reduced gradually to 1248 kN (280 kips) as the column was pushed to a drift ratio of +9.1%; where the test was stopped.

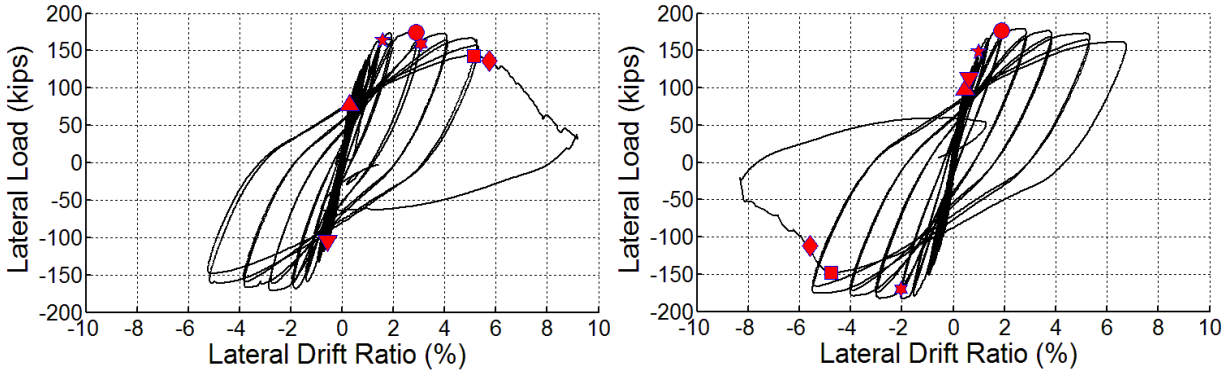

Figure 5 - Lateral load versus drift response of CS60 (left) and CS80 (right)

Similarly ot CS60, the initiation of lateral-strength loss of column CS80 was associated with a reduction in lateral load resistance accompanied with the opening of large shear cracks. Column CS80 lost lateral strength just prior to loss of axial capacity at a drift ratio of -4.6% as the column was being pushed to the first excursion to a drift ratio of -7.0% (Figure 5). Beyond a drift ratio of -4.6%, the column was no longer able to resist the target axial load of 1646 kN (370 kips) and that load was reduced gradually to 1023 kN (230 kips) as the column was pushed to a drift ratio of -8.2%; where the test was stopped.

The failure mode observed in both CS60 and CS80 columns was typical of a flexure-shear critical mode. In both specimens, the initiation of axial failure came shortly after the columns lost their lateral strength. Shear cracks that formed in the plastic hinge regions degraded the concrete core and the aggregate interlock mechanism leading the members to lose their lateral strength (Figure 6). The relatively high axial load in the order of 30%, crushed the already degraded plastic hinge generating sliding across the critical shear crack leading to axial failure. No buckling was observed in the longitudinal reinforcement up to the start of axial failure in either of the specimens (Figure 6).

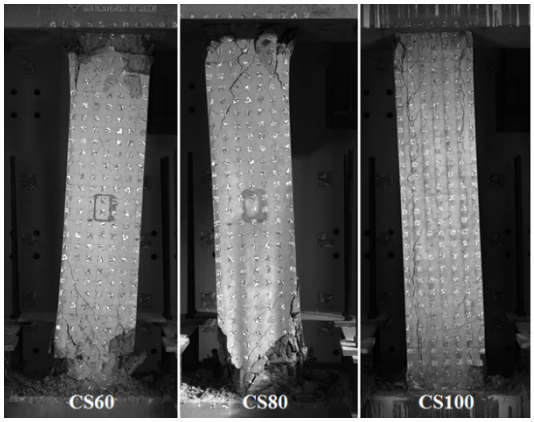

Figure 6 – Columns at failure

A stable response up to a drift ratio of 4% is generally considered to be a minimum performance objective for collapse prevention at the Maximum Considered Earthquake (MCE) hazard level. Both CS60 and CS80 showed comparable lateral-load behavior and remained stable beyond two cycles at a drift ratio of 5.5%. Mechanical properties of the reinforcement did not dictate major differences between the behaviors of the two specimens. The Grade 80 reinforcement preserved the integrity of the concrete core and shear transfer mechanisms to the same high demand levels as the conventional Grade 60 reinforcement.

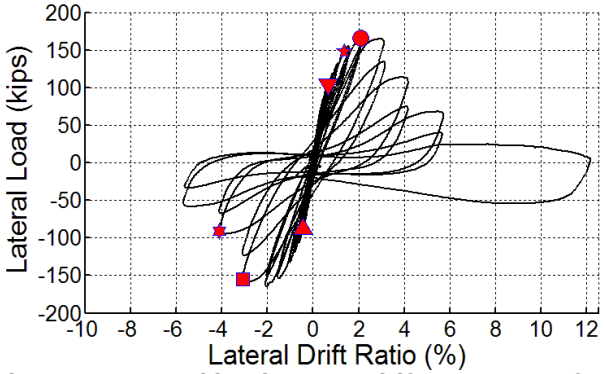

Figure 7 - Lateral load versus drift response of CS100

Column CS100 showed a comparable behavior to columns CS60 and CS80 up to a drift ratio of 1.5% (Figure 7). The crack pattern in the CS100 was similar to those of the other two columns until the end of the 1.5% drift cycles. Just after those drift cycles, longitudinal hairline cracks formed in the plastic hinge regions at the location of the outer longitudinal bars. These cracks became more noticeable at the end of the 2.0% drift cycles. At the end of first cycle towards a drift ratio of -3.0%, severe longitudinal cracks spread over the height of the column and were associated with bond degradation at the longitudinal bars. The initiation of lateral-strength loss was determined at that drift ratio of -3.0% as column lateral strength dropped significantly in subsequent cycles. The column was cycled up to, and through the 5.5% drift cycles, as its lateral strength dropped to 142 kN (32 kips; 18.9 % of peak strength). The column was then pushed monotonically to a drift ratio of +12% drift without loss of axial strength and while the lateral strength dropped to 58 kips (13 kips; 7.7% of peak lateral strength). The bond splitting failure released longitudinal bar stresses as well as the imposed shear forces on the column, which protected the concrete core from the shear/axial failure mode observed in the other two columns (Figure 6).

4. Demands on Bars

Strain gauges installed on corner longitudinal bars at both ends of each column provided strain measures at the point of highest demand. Figure 8 illustrates the maximum strain gauge measurements from all longitudinal-bar gauges at each drift target for each column. The #10 (32 mm) 420 MPa (Grade 60) bars used as longitudinal reinforcement in CS60 had an average yield strain of 0.0023 as measured from coupon tests. This strain was reached at a drift ratio of +1.6%, in the first cycle toward a drift target of 2.0%. The #9 Grade 80 bars used as longitudinal reinforcement in CS80 had an average yield strain of 0.0027. This strain was achieved at the end of the first cycle toward a drift ratio of 1.0%. The longitudinal bars in the CS100 specimen reached their average yield strain of 0.0035 at the end of the first cycle toward a drift ratio of 1.0%. As can be seen Figure 8, the 550 MPa (Grade 80) longitudinal bars in CS80 saw significantly larger strains at any drift level, and were up to 65% higher than those in longitudinal bars of CS60. Owing to the lower fracture strains of the higher grade bars, the longitudinal bars in CS80 reached 16.4% of their fracture strain at the end of the drift cycles to 5.5%, while longitudinal bars in CS60 only reached 8.7% of their fracture strain. The longitudinal bars in CS100 did not reach as high strains as those in the other two columns due to the premature bond splitting failure. However, longitudinal bars in CS100 had significantly higher strains (about 25% higher than in CS80 and 100% higher than in CS60) up to the end of the 1.5% drift cycles and prior to significant loss of bond. Similarly, higher strains were observed in the transverse reinforcement in the specimens with higher strength reinforcement.

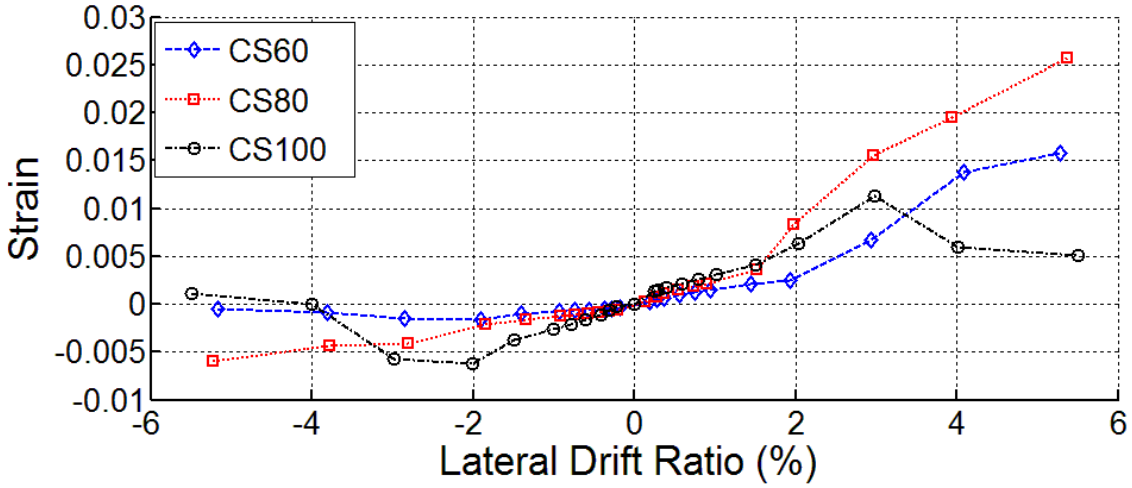

Figure 8 – Maximum measured strains at the first cycle to drift targets for each specimen

5. Conclusions

Three full-scale concrete columns satisfying most of the provisions of ACI 318-14 for Special Moment Resisting Frames were tested under constant axial load and cyclic lateral loading until loss of axial strength or until significant degradation of the lateral resistance. Columns were designed to have almost identical flexural capacity and associated shear demands and to impart large demands on the transverse reinforcement. Columns had large shear stresses generated by a high longitudinal reinforcement ratio and large confinement demands generated by a relatively large compressive axial load. Columns were reinforced with longitudinal and transverse bars of varying grades. Column CS60 was reinforced with Grade 60 A706 (420MPa) bars, column CS80 was reinforced with Grade 80 A706 (550 MPa) bars, and column CS100 was reinforced with newly developed Grade 100 and 120 bars (690 MPa and 830 MPa).

Columns CS60 and CS80 showed comparable lateral-load behavior and remained stable beyond two reversed cycles at a lateral drift ratio of 5.5%, having an envelope of the lateral load versus drift response similar for both columns. Both columns, sustained shear failures at about the same drift level, which indicates that 550 MPa (Grade 80) reinforcement maintained the integrity of shear transfer mechanisms as well as the 420 MPa (Grade 60) reinforcement. The two specimens failed axially almost immediately after the initiation of shear failure. Axial collapse occurred when the shear damaged area could no longer sustain the imposed axial load. CS60 and CS80 maintained the integrity of shear transfer mechanism up to relatively large deformations with the mechanisms of shear degradation performed similarly for both columns independent of the yield strength of the reinforcing bar. Column CS80 had up to 65% higher strain demands in the longitudinal reinforcement than Column CS60. Owing to the lower fracture strain of the 650 MPa (Grade 80) bars used, the 550 MPa (Grade 80) longitudinal bars reached 16.4% of their fracture strain, as compared with the 420 MPa (Grade 60) longitudinal bars reaching only 8.7% of their fracture strain.

Up to a lateral drift ratio of 1.5% column CS100 had higher strain demands in the longitudinal reinforcement than the other two columns, up to 10% larger than those in column CS60 at a given drift level. Bond degradation initiated in column CS100 after drift ratio of 1.5%. The ACI 318-14 code does not have an explicit requirement to check for bond failure due to steep moment gradients. As the profession moves towards higher strength reinforcing bars, such a check becomes more critical and should be introduces in the design code.

6. Acknowledgment

The authors wish to express their gratitude and sincere appreciation to Nucor Inc. Seattle and CRSI for financing this research work and for their valuable assistance in making this project a reality.

7. References

ACI 318-14 Building Code Requirements for Structural Concrete and Commentary. 2014: American Concrete Institute.

ASTM A370-14, Standard Test Methods and Definitions for Mechanical Testing of Steel Products, ASTM International, West Conshohocken, PA, 2014, www.astm.org

ASTM A706 / A706M-14, Standard Specification for Deformed and Plain Low-Alloy Steel Bars for Concrete Reinforcement, ASTM International, West Conshohocken, PA, 2014, www.astm.org

ASTM C39 / C39M-14a, Standard Test Method for Compressive Strength of Cylindrical Concrete Specimens, ASTM International, West Conshohocken, PA, 2014, www.astm.org

ASTM E8 / E8M-13a, Standard Test Methods for Tension Testing of Metallic Materials, ASTM International, West Conshohocken, PA, 2013, www.astm.org

Sokoli, Drit, Shekarchi, William, Buenrostro, Elliud, Ghannoum, Wassim M., “Advancing Behavioral unerstanding and damage evaluation of concrete members using high-resolution digital image correlation data”, *Earthquakes and Structures*, 2014. **7**(5).